Published in final edited form as:
Science. 2017 June 09; 356(6342): 1076–1080. doi:10.1126/science.aaj2067.

Local enhancers of Type 2-mediated macrophage activation and proliferation promote tissue repair

Carlos M. Minutti[1,2,3], **Lucy H. Jackson-Jones**[#3], **Belén García-Fojeda**[#1,2], **Johanna A. Knipper**[3], **Tara E. Sutherland**[3,8], **Nicola Logan**[3], **Emma Rinqvist**[3], **Raquel Guillamat-Prats**[2,4], **David A. Ferenbach**[3], **Antonio Artigas**[2,4], **Cordula Stamme**[5], **Zissis C. Chroneos**[6,7], **Dietmar M. Zaiss**[3], **Cristina Casals**[1,2,*], and **Judith E. Allen**[3,8,*]

[1]Department of Biochemistry and Molecular Biology I, Complutense University of Madrid, 28040-Madrid, Spain

[2]Centro de Investigación Biomédica en Red de Enfermedades Respiratorias (CIBERES); Instituto de Salud Carlos III, 28029-Madrid, Spain

[3]School of Biological Sciences & School of Clinical Sciences, University of Edinburgh, Edinburgh EH9 3FL, UK

[4]Critical Care Centre, Corporació Sanitària Universitària Parc Taulí, Universitat Autònoma de BarcelonaParc Taulí 1, 08208-Sabadell, Spain

[5]Division of Cellular Pneumology, Research Center Borstel, Leibniz-Center for Medicine and Biosciences 23845, Borstel and Department of Anesthesiology, University of Lübeck, 23583 Lübeck, Germany

[6]Pulmonary Immunology and Physiology Laboratory, Department of Pediatrics, The Pennsylvania State University, College of Medicine, Hershey PA 17033, USA

[7]Microbiology and Immunology The Pennsylvania State University, College of Medicine, Hershey PA 17033, USA

[8]Faculty of Biology, Medicine & Health, Wellcome Centre for Cell-Matrix Research & Collaborative Centre for Inflammation Research, Manchester Academic Health Science Centre, University of Manchester, Manchester M13 9PT United Kingdom

[#] These authors contributed equally to this work.

Abstract

[*]Correspondence to: judi.allen@manchester.ac.uk, ccasalsc@ucm.es.

Author Contributions

C.M.M. designed and performed research, analyzed and interpreted data and wrote the manuscript; L.H.J-J., B.G-F, T.E.S., J.A.K., N.L. and E.R. performed research, contributed to experimental design and manuscript preparation; R.G-P. performed research; D.A.F., A.A., C.S. and Z.C. contributed tools, provided expertise and edited the manuscript; D.M.Z. contributed to project funding, provided expertise and edited the manuscript; C.C. and J.E.A funded and designed the research, organized the project and analyses, and wrote the manuscript. All authors reviewed and approved the final version of the manuscript.

Competing financial interests

The authors declare no conflict of interest

Europe PMC Funders Author Manuscripts

The type 2 immune response controls helminth infection and maintains tissue homeostasis but can lead to allergy and fibrosis when improperly controlled. We reveal the existence of local tissue-specific enhancers of type 2 mediated-macrophage activation. In the lung, surfactant protein A (SP-A) enhanced IL-4-dependent proliferation and activation of alveolar macrophages, accelerating parasite clearance and reducing pulmonary injury following infection with a lung-migrating helminth. In the peritoneal cavity and liver, C1q enhancement of type 2 macrophage activation was required for liver repair following bacterial infection, but resulted in tissue fibrosis following peritoneal dialysis. Both SP-A and C1q generated their effects on macrophages via the unconventional myosin18A that acts as a cell surface receptor. We conclude that the structurally related defense collagens SP-A and C1q are tissue-specific factors that act through myosin18A to license local type 2 responses with consequences for parasite control, tissue repair, and fibrosis.

The type 2 cytokines IL-4 and IL-13, which signal through IL-4Rα, trigger a specialized macrophage phenotype (M(IL-4)) (1) that promotes control of helminth infection (2) and tissue repair (3, 4). M(IL-4)s also contribute to pathology associated with type 2 immunity including allergy, asthma, and fibrosis (4). However, little is known about tissue-specific factors that might promote both beneficial and detrimental actions of M(IL-4)s.

In the lung, alveolar macrophages (aMϕs) together with the respiratory epithelium are covered by pulmonary surfactant, a lipid-protein network in which surfactant protein A (SP-A) constitutes the major protein component (5). SP-A is a versatile recognition protein (5) that is a member of a group of secreted soluble defense collagens that include the first component of the complement system (C1q), collectins (e.g., SP-A, SP-D, mannan-binding lectin), ficolins, and adiponectin (6). Because of its abundance and known role in immune defense (5), we chose to ask whether SP-A was involved in the local regulation of M(IL-4) effector function in the lung.

M(IL-4)s have a critical role in lung repair following infection with the lung-migrating nematode *Nippostrongylus brasiliensis (Nb)* (3). We therefore infected WT, IL-4Rα-deficient and SP-A-deficient mice with *Nb* infective larvae. Larvae migrate to the lung where they mature for ~2 days, and reach the small intestine by d3 post infection. The type 2 response peaks at days 6-7 after inoculation. We observed an up-regulation of SP-A mRNA (Fig. 1A) and protein (Fig. 1B) in lungs of *Nb* infected C57BL/6 mice at d6, which was dependent on IL-4Rα. Consistent with a role for SP-A during type 2 immunity to nematode infection, SP-A-deficient mice had increased adult worm burden and egg output (Fig. 1C,D) and significantly impaired lung repair processes (Fig. 1E, F). This failure to heal was associated with a failure to up-regulate tissue-repair related gene *Col1a1* (Collagen, type I, alpha 1) (Fig. 1G) and increased expression of *Mmp12*, an extracellular matrix-degrading enzyme (Fig. 1H). Greater lung damage in SP-A-deficient mice was evidenced by increased numbers of RBCs and neutrophils in bronchoalveolar lavage (BAL) at d6 (Fig. 1I, J). The absence of SP-A resulted in reduced protein expression of the M(IL-4) markers RELMα (Fig. 1K), Ym1 (Fig. 1L), and Arginase (not shown) in aMϕs isolated from BAL and lungs (Fig. S1A). Secretion of RELMα and Ym1 protein into the alveolar fluid (Fig. S1B) was also reduced in SP-A-deficient mice compared to WT mice.

Consistent with the known ability of IL-4 to cause macrophage proliferation during helminth infection (7), aMϕs from WT mice exhibited significant proliferation (Fig. 1M, N) and highly increased aMϕs numbers (Fig. S1C) d6 following *Nb* infection. However, SP-A-deficient mice failed to exhibit significantly enhanced Mϕ proliferation in BAL (Fig. 1M, N) and lung tissue (Fig. S1D) resulting in significantly fewer total Mϕ numbers relative to WT mice (Fig. S1C). There was no evidence that differences were due to a failure of SP-A-deficient mice to mount appropriate adaptive T_H2 responses (Fig. S1E & F) or local type 2 cytokine responses (Fig. S1G). Importantly, aMϕs from uninfected SP-A-deficient mice were normal in number, phenotype and ability to respond to IL-4 ex vivo (Fig. S2A-D).

To ascertain if defects in SP-A-deficient mice were due to defective IL-4Rα responsiveness in vivo, WT and SP-A-deficient mice were injected intra-peritoneally (ip*)* with IL-4 complex (IL-4c). IL-4c delivery increased the amount of SP-A protein in BAL (Fig. 1O) and lung (not shown) in WT mice, and decreased IL-4Rα expression in both WT and SP-A-deficient aMϕs (Fig. 1P). IL-4c delivery induced proliferation and M(IL-4) markers in aMϕs isolated from BAL (Fig. 1Q,R and Fig. S3A) and lungs (Fig. S3B, C) of WT but not SP-A-deficient mice, reflected by diminished secretion of RELMα and Ym1 to the alveolar fluid in SP-A-deficient mice (Fig. S3D).

Enhancement of M(IL-4)s may underlie the previously reported contribution of SP-A to tissue integrity in other models of acute lung injury (8, 9). The pro-type 2 effects we report here contrast with reports that associate SP-A with protection in asthma (10). However, in addition to promoting M(IL-4) and proliferation of macrophages, the anti-inflammatory properties of SP-A (5, 6, 8, 9, 11) may suppress the strong inflammatory responses that are responsible for more severe asthma. Our data are supported by the finding that SP-D-deficient mice, which lack SP-A (12), also have reduced M(IL-4) responsiveness (13).

To determine whether SP-A acts directly on aMϕs, we first tested the ability of adherence-purified macrophages from the alveolar and peritoneal spaces to proliferate in vitro in response to 1 μg/ml of IL-4; aMϕ exhibited significant proliferation, but peritoneal macrophages (pMϕ) failed to proliferate despite expressing M(IL-4) activation markers (Fig. S4A). We then tested the ability of SP-A to enhance IL-4 treatment and included C1q as a control because it is a defense collagen structurally homologous to SP-A (5, 6). We found that SP-A, but not C1q, significantly boosted IL-4-mediated aMϕ proliferation and M(IL-4) markers (Fig. 2A). IL-4Rα-deficient aMϕ showed no proliferation or activation when stimulated with IL-4 (1 μg/ml) in the absence or presence of SP-A (Fig. S4B). Notably, SP-A significantly enhanced proliferation and activation induced by IL-4 in both human (Fig. S4C) and rat aMϕs (Fig. S4D).

To our surprise C1q, but not SP-A, significantly increased IL-4-mediated proliferation and M(IL-4) marker expression in pMϕ (Fig. 2A). To verify these findings in vivo, IL-4c was delivered to C1qa-deficient mice. Consistent with the in vitro studies, mice lacking C1q exhibited reduced IL-4-dependent activation and proliferation in pMϕ but not aMϕ (Fig. 2B). Similar to SP-A in the lung (Fig. 1O), C1q levels increased in the peritoneal fluid after IL-4c delivery (Fig. S5A), indicating that IL-4 drives production of a local signal to amplify its effect on tissue macrophages. Importantly, the pMϕ phenotype, number, and ability to

respond to IL-4 ex vivo are normal in C1qa-deficient mice (Fig. S5 B-F). Thus, SP-A and C1q were induced by IL-4 in the lung and peritoneal cavity, respectively, where they acted to enhance proliferation and M(IL-4) activation in a tissue-specific manner.

To determine which receptor mediates SP-A effects on IL-4-stimulated aMϕs, we inhibited known receptors for SP-A (5). We observed that the blockade of Myosin18A (Myo18A, *aka* SP-R210), but not signal inhibitory regulatory protein α (SIRPα) or calreticulin (*aka* cC1qR), abrogated SP-A-mediated enhancement of IL-4-induced arginase activity in rat aMϕs (Fig. S6A). Blockade or RNA silencing of Myo18A consistently abolished SP-A-mediated enhancement of IL-4-induced proliferation and activation of mouse (Fig. 2C), human (Fig. S6B) and rat (Fig. S6C) aMϕs. Myo18A is an unconventional myosin that does not operate as a traditional molecular motor, having both intracellular and cell-surface locations (14), and was recently defined as CD245 (15). Immune activation results in Myo18A localization on the cell surface, where it binds to the collagen-like domain of SP-A (6, 16) and we confirmed that an intact collagen-like domain is required to enhance IL-4-mediated type 2 responses (Fig. S6D).

Because C1q is structurally homologous to SP-A in its supra-trimeric assembly and collagen tail (5, 6), we addressed whether Myo18A was also responsible for the actions of C1q. Indeed, blockade of Myo18A prevented C1q enhancement of IL-4 driven activation and proliferation of peritoneal Mϕ (Fig. 2C). In vitro, IL-4 promoted Myo18A localization on the cell surface of both aMϕ and pMϕ (Fig. S7A, B), which was maximal 24 hours after stimulation. Cell surface expression of Myo18A was similarly observed in vivo following IL-4c delivery (Fig. 2D), independent of the presence or absence of SP-A or C1q. We confirmed the role of Myo18A in vivo by intranasal or intraperitoneal delivery of anti-Myo18A antibody. Receptor blockade significantly reduced IL-4-induced proliferation of aMϕ and pMϕ (Fig. 2D), as well as M(IL-4) activation of aMϕ and pMϕ, and secretion of RELMα and Ym1 to the alveolar and peritoneal fluid (Fig. S7C-F). Thus, Myo18A receptor blockade in the lung or peritoneal cavity phenocopied SP-A or C1qa deficiency, respectively. Taken together, these data suggest that Myo18A is a common receptor or co-receptor for defense collagens present on aMϕs and pMϕs, which determines macrophage capacity to respond to IL-4 and whose cell surface expression is itself induced by IL-4. Myo18A lacks a trans-membrane domain (14), and thus must act in concert with transmembrane co-receptors for signal transduction that likely impart tissue-specificity.

The relevance of C1q as a local factor to enhance type 2 responses is supported by the fact that unlike most other complement components, the majority of C1q is produced by myeloid cells in peripheral tissues (17). To determine the physiological relevance, we evaluated the role of C1q in a murine model of peritoneal fibrosis (18). Peritoneal fibrosis is a frequent and serious consequence of peritoneal dialysis (19) associated with alternatively activated macrophages in both humans and mice (18–20). We administered Dianeal-PD4, a clinically-used lactate-based dialysate, every other day for 28 days to WT, C1qa- and IL-4Rα-deficient mice. In WT, but not in C1qa-deficient mice, Dianeal-PD4 treatment provoked the induction of C1q (Fig. 3A) and morphologic changes in tissue sections of the parietal peritoneum, showing significant enlargement of the submesothelial zone caused by collagen deposition (Fig. 3B, C). Dianeal-PD4 treatment induced markers of fibrosis including collagen mRNAs

(*Col1a1* and *Col3a1*) (Fig. 3D), alpha-smooth muscle actin (*Acta2)* (Fig. 3E), and vascular endothelial growth factor *(Vegf)* (Fig. 3F). Significant upregulation of these markers was not observed in C1qa-deficient mice (Fig. 3D-F). Conversely, *Mmp12* mRNA was up-regulated in C1qa-deficient mice relative to WT mice (Fig. 3G) consistent with monocyte infiltration (Fig. 3H) (21) and an anti-inflammatory role for C1q (22). Dianeal-PD4 treatment also induced intracellular expression and protein secretion of the M(IL-4) markers RELMα, Ym1, and Arg (Fig. 3I-K) and moderate proliferation of pMϕs (Fig. 3L) in WT but not C1qa-deficient mice. Despite the clear induction of M(IL-4) markers by PD4 delivery and their dependence on C1q, responses of IL-4Rα-deficient mice were equivalent to WT mice (Fig. 3A-L). Although initially surprising, Dianeal-PD4 is a lactate-based solution, and lactate can induce M(IL-4) markers by acting downstream of IL-4Rα through stabilization of HIF1α protein (23). Indeed, we observed that the induction of proliferation and M(IL-4) markers following Dianeal-PD4 delivery was essentially absent in mice lacking HIF1α in macrophages (Fig. S8). Together, our data indicate that C1q significantly amplifies peritoneal fibrosis by promoting a type 2 macrophage phenotype driven by lactate and dependent on HIF1α. These results are consistent with human studies in which C1q is strongly associated with increased fibrosis of skeletal muscle (24).

Critically, we needed to ascertain whether C1q functioned as a type 2 enhancer in tissues beyond the peritoneal cavity and settings clearly dependent on IL-4Rα. We thus assessed Myo18A expression on the cell surface of resident macrophages from mice treated with or without IL-4c (Fig. 4A). Consistent with our functional data, Myo18A was expressed in macrophages from the lung and peritoneal cavity, as well as in liver, spleen and adipose tissue, and significantly increased by IL-4 exposure. In contrast, there was an absence of Myo18A on pleural cavity macrophages, which explained our failure to identify a role for C1q in the pleural cavity following IL-4c delivery (Fig. S9). Given that IL-4 enhanced Myo18A expression on liver macrophages, we assessed liver macrophages from C1qa-deficient mice and found they had significantly lower levels of proliferation and activation compared to WT mice following IL-4c delivery (Fig. 4B). Importantly, we observed C1q upregulation in the liver of IL-4c treated mice (Fig. 4C). Of relevance, the number and phenotype of liver Mϕs are normal in C1qa-deficient mice (Fig. S10). Antibody blockade of Myo18A following IL-4 treatment of isolated liver macrophages verified that C1q generated its effects through Myo18A (Fig. S11). We thus sought a model in which M(IL-4)s in the liver played a substantive role.

Infection of the liver by the gram-positive bacteria *Listeria monocytogenes* (Lm) causes necroptotic death of resident liver Mϕs (Kupffer cells) followed by recruitment of monocytes, which control Lm infection (25) and repopulate the liver Mϕ population (26). Following an initial type 1 response, a type 2 response begins at 3 dpi with IL-4-mediated activation and proliferation of liver Mϕs acting to repair infection damage (26). To ascertain the relevance of C1q and confirm the role of IL-4Rα in this process, we infected WT, C1qa- and IL-4Rα-deficient mice with Lm and performed sample analysis at 3.5 dpi. Lm infection induced IL-4Rα-dependent up-regulation of C1q mRNA in liver (Fig. 4C) while liver macrophages exhibited enhanced expression of RELMα and Ym1 (Fig. 4D) and proliferation (Fig. 4E), which were dependent on both IL-4Rα and C1q. Consistent with the requirement for basophil-derived IL-4 in Lm-induced liver macrophage proliferation (26),

we observed increases in IL-4 and IL-13 cytokines in liver homogenates (Fig. S12). C1q and IL-4Rα deficiency were associated with increased liver injury as assessed by liver transaminases in blood (Fig. 4F) and a failure to up-regulate tissue-repair related genes (*Acta2* and *Col1a1*) (Fig. 4G). Notably, at 3.5 dpi, liver bacterial burden was higher in WT than in C1qa- or IL-4Rα-deficient mice (Fig. 4H), which had increased numbers of recruited monocytes (Fig. 4I) and higher iNOS expression in monocytes ($CD11b^+$ $Ly6C^+$) and liver Mϕ ($CD11b^+$ $F4/80^+$) (Fig. 4J). These data suggest that C1q, through its ability to orchestrate IL-4Rα-dependent type-2-mediated responses, not only decreases the strong bactericidal and pro-inflammatory capacity of monocyte-derived macrophages, thus limiting liver injury, but also promotes the return to homeostasis (Fig. 4D-J).

M(IL-4)s have recently emerged as important players in homeostatic processes (27), but IL-4Rα-dependent pathways are amplified during helminth infection with uncontrolled amplification leading to fibrosis (4, 28, 29). Our data show that IL-4 drives production of local specific factors (SP-A and C1q) and expression of their receptor (Myo18A) on the macrophage surface for full M(IL-4) activation and proliferation (Fig S13). These findings reveal the existence within distinct tissues of an amplification system needed to permit effective type 2 functionality. SP-A and C1q are typically produced by alveolar epithelial type II and myeloid cells, respectively, indicating that several different cell types must respond to IL-4 for signal amplification.

The study raises a number of critical questions. What are the Myo18A co-receptors that mediate tissue-specificity? What factors negatively regulate or stop the positive M(IL-4) loop? What are the intracellular signaling pathways regulated by Myo18A and its co-receptors? Critically, SP-A, C1q, and Myo18A are highly conserved across mammalian species, and we have demonstrated the ability of SP-A and Myo18A to enhance human alveolar M(IL-4) proliferation. Thus the answers to these questions have the potential to provide entirely new directions for tissue-specific targeting of type 2 macrophage activation-driven pathologies, such as fibrosis (4), or to promote local repair.

Methods

Proteins

Surfactant protein A was isolated from BAL of patients with alveolar proteinosis using a sequential butanol and octylglucoside extraction (11, 30–33). The purity of SP-A was checked by one-dimensional SDS-PAGE in 12 % acrylamide under reducing conditions and mass spectrometry. The oligomerization state of SP-A was assessed by electrophoresis under non-denaturing conditions (31–33), electron microscopy (33), and analytical ultracentrifugation as reported elsewhere (32). SP-A consisted of supratrimeric oligomers of at least 18 subunits. Each subunit had a relative molecular mass (Mr) 36 kDa. Recombinant human SP-A1 ($SP\text{-}A1^{hyp}$) was expressed in insect cells and purified from the medium by mannose affinity chromatography (31, 32). The stability of $SP\text{-}A1^{hyp}$ collagen domain was assessed by circular dichroism (31, 32) and differential scanning calorimetry (32). The oligomerization state of $SP\text{-}A1^{hyp}$ was evaluated by electrophoresis under non-denaturing conditions (31, 32) and analytical ultracentrifugation (32). $SP\text{-}A1^{hyp}$ consists of trimers and hexamers. The endotoxin content of native or recombinant human SP-A was < 0.1 endotoxin

units /mg of SP-A as determined by Limulus amebocyte lysate assay (GenScript, Piscataway, New Jersey). The microbicidal activity of native and recombinant human SP-A against *Escherichia coli* J5 was evaluated by bacterial killing assays as described previously (30). Levels of mouse SP-A from BAL, pleural exudate, or lung tissue were detected by western-blot analysis as reported elsewhere (11, 30–33). Native human C1q was obtained from Abcam (Cambridge, UK). C1q consists of octadecameres with a Mw 410 kDa.

Experimental animals

C57BL6 WT and gene-targeted mice were used in this study. SP-A (*Sftpa1*$^{-/-}$) (34), C1q (*C1qa*$^{-/-}$) (35), IL-4Rα (*Il4ra*$^{-/-}$) (36) and myeloid-specific HIF-1α (*Hif1a*$^{flox/flox}$;*LysMcre*$^{+/-}$) (37) deficient mice and WT mice were bred and maintained at the University of Edinburgh in specific-pathogen free conditions. Sex-matched mice were 6-8-weeks old at the start of the experiment, and all mice were housed in individually ventilated cages. *Sftpa1*$^{-/-}$ and *Sftpa1*$^{+/+}$ littermates were genotyped using specific primers (Supplementary Table 1) and used for *N. brasiliensis* infection experiments. Mice were not randomized in cages, but each cage was randomly assigned to a treatment group. Investigators were not blinded to mouse identity during necropsy; however, the analysis of adult worms, eggs in faeces, lung and peritoneal pathology were performed in a blinded fashion. Experiments were performed in accordance with the United Kingdom Animals (Scientific Procedures) Act of 1986 and the Spanish guidelines for experimental animals. All researchers were accredited for animal handling and experimentation by the UK and Spanish government Home Office. Dispensation to carry out animal research at The University of Edinburgh was approved by the University of Edinburgh Animal Welfare and Ethical Review Body and granted by the UK government Home Office; as such all research was carried under the project licenses PPL60/4104, PPL70/8548 and PPL70/8470. Sample size was calculated on the basis of the number of animals needed for detection of macrophage proliferation in WT mice, based on published experiments (38–40). Data was not excluded under any circumstances.

Sprague Dawley rats (~350 g) were purchased from Harlan (Indianapolis, IN). All animal experiments were fully compliant with the regulations set by the local ethical committee. Animals were treated according to the Directive 2010/63/EU of The European Parliament and the Spanish act RD53/2013 of 8th February 2013 on protection of animals used for experimentation and other scientific purposes.

Nippostrongylus brasiliensis infection

Mouse-adapted *N. brasiliensis* was maintained by serial passage through C57BL/6 mice, as described previously (41). Mice were infected subcutaneously with 250 or 400 *N. brasiliensis* third-stage larvae. Analysis of samples was performed at day 6 post-infection. Egg output was analyzed in faeces and adult worm burden was determined by removing the small intestine and exposing the lumen by dissection. For macrophage proliferation analysis, mice were injected with 100 μl of 10 mg/ml BrdU in Dulbecco's phosphate buffered saline 3h before experimental end-point. The lungs and pleural cavities were washed to obtain the bronchoalveolar lavage (BAL) and pleural exudate. Subsequently, the right lung was perfused and fixed for histology. Alternatively, one section of the left lung was stored for

mRNA quantification; another section was homogenized to obtain single cell suspensions for flow cytometry analysis, and a third section was stored for SP-A quantification. In this case, lung tissue was homogenized in HBSS containing protease inhibitor cocktail (Sigma). SP-A was detected in both lung homogenates and BAL by western blot analysis using an anti-mouse SP-A (GeneTex, Inc, Irvine, CA). SP-A levels were normalized by BAL volume or GAPDH. Only samples on which the same BAL volume was recovered were used for SP-A quantification.

BAL cells were obtained by washing the lung with Dulbecco's phosphate buffered saline containing 0.5% BSA (m/v). Cells from pleural or peritoneal exudate were obtained by washing either pleural or peritoneal cavity with RPMI 1640 containing 2 mM L-glutamine, 200 U/ml penicillin, 100 μg/ml streptomycin. Single cell suspensions of thoracic lymph node tissue were re-stimulated *ex vivo* with *N. brasiliensis* excretory secretory antigen (42) (1 μg/ml) or anti-CD3 (1 μg/ml), and cell supernatants were analysed by ELISA 72 h later.

Listeria monocytogenes infection

Listeria monocytogenes infections were performed as previously described (26). Briefly, frozen stocks of *Listeria monocytogenes* (Lm10403s) were thawed and then diluted in fresh Brain-Heart-Infusion (BHI) medium to reach mid-log growth phase. Mice were intravenously injected via the lateral tail vein with 1 x10^4 *L. monocytogenes* c.f.u. suspended in 200 μl of PBS. Analysis of samples was performed at day 3.5 post-infection. The livers were perfused *in situ* with phosphate-buffered saline (PBS) before collection. For macrophage activation and proliferation analysis, mice were injected with 100 μl of 10 mg/ml BrdU in Dulbecco's phosphate buffered saline 3h before experimental end-point. One section of the liver was homogenized to obtain single cell suspensions for flow cytometry analysis, a second section of the liver was stored for mRNA quantification; a third section was stored for cytokine quantification by ELISA; and a fourth section was homogenized to analyze bacterial burden. To analyze cytokine secretion by ELISA, the liver tissue was weighed before homogenization in Hank's balanced salt solution (HBSS) containing protease inhibitor cocktail. To quantify bacterial burden, serial dilutions of cell suspensions in PBS were plated on BHI agar plates. After 24 hr of incubation at 37°C, colony-forming units were counted. To analyze liver damage, blood was collected from the inferior vena cava and alanine transaminase (ALT) and aspartate transaminase (AST) levels were determined in the serum.

Peritoneal fibrosis model

Peritoneal fibrosis was induced by continuous administration of Dianeal PD-4 (Baxter, Deerfield, Illinois), as described previously (18) with slight modifications. Mice received a total of 5 or 14 injections of 500 μl (~200 ml/kg) of Dianeal PD-4 (ip) on alternate days. Animals were sacrificed a day after the last delivery. The right section of the parietal layer of the peritoneum was collected for histology analysis. The left section of the peritoneum was stored in RNAlater for subsequent analysis. Peritoneal macrophages were isolated from the peritoneal cavity as described below.

Histology

The right lung lobes were perfused and fixed with 10% neutral buffered formalin, incubated overnight and transferred to 70% ethanol. Lungs were paraffin-embedded, sectioned and stained with H&E. Linear means intercept (Lmi) method was used to quantify emphysema like damage (43). To calculate Lmi, 20 random non-overlapping fields (magnification x200) per H&E stained lung sample were taken. Six horizontal lines were drawn across each image (ImageJ 1.44) and the total number of alveolar wall intercepts counted per line. The length of each line was then divided by the number of intercepts to give the Lmi value. Images that included large bronchi and vessels were avoided and analysis was performed in a blinded and randomised fashion. With respect to histological analysis of the peritoneum tissue, the right parietal layer of the peritoneum was fixed with 10% neutral buffered formalin, incubated overnight and transferred to 70 % ethanol. Subsequently, peritonea were paraffin-embedded, sectioned and stained for Masson's trichrome. The thickness of the submesothelial compact zone was measured using ImageJ and this value was used to score the extent of peritoneal fibrosis. Five independent (×200) images were taken to examine the overall section. For each image, six horizontal lines were randomly drawn across the submesothelial compact zone to measure its thickness and the average value of each sample was used for analysis.

IL-4 complex delivery and *in vivo* blocking of Myo18A

IL-4 was delivered as a 2:1 molar ratio of recombinant mouse IL-4 (Peprotech) and anti-IL-4 mAb (clone 11B11; BioXcell,) (38, 39). For pulmonary macrophage analysis, mice were injected ip with IL-4 complex (IL-4c) containing 5 μg of IL-4 and 25 μg of 11B11, or PBS vehicle control on days 0 and 2. Simultaneously, 50 μg of anti-Myo18A antibody (44) or Rabbit IgG (R&D Systems) were delivered intra-nasally on days 2 and 3, and samples were collected on day 4. For studies of peritoneal macrophages, liver macrophages, and other tissue resident macrophage populations, mice received a single ip injection of 1 μg of IL-4 and 5 μg of 11B11, or PBS vehicle control. Anti-Myo18A neutralizing antibody or Rabbit IgG (100 μg) was delivered 2 hours before IL-4c injection and samples were collected 24 hours later. Mice received a pulse of BrdU 3 h before experimental end-point. Bronchoalveolar, pleural and peritoneal cavity lavages as well as lung and liver tissue collection were performed as described above.

RNA extraction and quantitative real-time PCR

A section of the left lung, liver or parietal peritoneum was stored in RNAlater (Ambion, Carlsbad, CA). Tissue was homogenised in Trizol (Invitrogen) with a TissueLyser (Qiagen, Hilden, Germany). Similarly, human alveolar macrophages were collected with Trizol, and RNA was prepared according to manufacturer's instructions. Reverse transcription was performed using 1 μg of total RNA, 50 U Tetro reverse transcriptase (Bioline, London, UK), 40 mM dNTPs (Promega, Fitchburg, WI), 0.5 μg Oligo dT15 (Roche, Basel, Switzerland), and RNasin inhibitor (Promega). Transcript levels of genes of interest were measured by real-time PCR with the Lightcycler 480 II system (Roche) using SYBR Green I Master kit and specific primers (Supplementary Table 2) as previously described (43). Transcript levels of C1qa mRNA were measured using Taqman Master kit and the primers Mm00432142

(Applied Biosystems), PCR amplification was analyzed using 2nd derivative maximum algorithm (LightCycler 480 Sw 1.5, Roche) and the expression of the gene of interest was normalized to a housekeeping gene *Rn18s*, *Rpl13a,* or *GAPDH*. In the case of human alveolar macrophages, cells from at least 8 humans were used for all groups.

Flow Cytometry

Single cell suspensions from left lung, liver and other tissues were prepared by digesting with 80 U/ml DNase (Life Technologies, Carlsbad, California) combined with 0.2 U/ml liberase TL (Roche) in HBSS at 37°C for 30 minutes. In some cases, liberase was combined with collagenase B (0.2 mg/ml) and D (0.4 mg/ml) (Roche). Tissue was homogenized by forcing through a 70 μM cell strainer. Cells from tissue homogenates, BAL, pleural exudate, and peritoneal cavity exudate were treated with red blood cell lysis buffer (Sigma) and counted using an automated cellometer T4 (Peqlab). Cells were incubated with Fc block (CD16/CD32 and mouse serum) and stained with fluorescent conjugated antibodies to CD19 (6D5), Siglec F (E50-2440), Ly6G (1A8), CD3 (17A2), CD45.2 (104), Ly6C (HK1.4), CD11c (N418), CD11b (M1/70), F4/80 (BM8), I-A/I-E (MHCII) (M5/114.15.), CD102 (3C4), GATA6 (D61E4), TER119 (TER-119) (eBioscience, Hatfield, UK; Biolegend, Cambridge, UK; or BD, Franklin Lakes, NJ), and unconjugated anti-Myo18A antibody (5 μg/ml) or isotype control followed by secondary reagents (Invitrogen). The following surface markers identified alveolar macrophages: lineage^{-} (CD19, Ly6G, CD3 and TER119), Ly6C^{-}, CD45.2^{+}, CD11c^{+} and SiglecF^{+}. Peritoneal and pleural, and liver macrophages as well as other tissue resident macrophages were identified as lineage^{-} (CD19, SiglecF, Ly6G and CD3), CD11c^{-}, Ly6C^{-}, CD45.2^{+}, CD11b^{+} and F4/80$^{+\text{ or high}}$ (38). ILC2 cells were identified as lineage^{-} (CD3, CD11b, CD11c, FcεR1, CD19, and NK1.1) CD90^{+} ICOS^{+} CD45^{+} cells. T helper cells were identified as CD45^{+}, CD3^{+} and CD4^{+}. Neutrophils were identified as CD45^{+}, CD11b^{+} and Ly6G^{+}. Monocytes were identified as CD45^{+}, CD11b^{+} and Ly6C^{+}.

Following surface staining, cells were fixed with 2% paraformaldehyde in Dulbecco's phosphate buffered saline for 20 min at room temperature, permeabilized with Perm wash (BD), and then stained with anti-RELMα, biotinylated anti-Ym1, APC-conjugated anti-Arg-1 (R&D Systems, Minneapolis, MN), or isotype control followed by secondary reagents (Invitrogen). For detection of Ki67 and measurement of BrdU incorporation, cells were stained for surface markers, then fixed and permeabilized using FoxP3 staining buffer set (eBioscience), and subsequently stained with Ki67 set (BD clone BV56) or anti-BrdU (BU20a) for 30 min at room temperature. Cells were incubated first with or without DNase for 30 mins at 37ºC before staining with anti-BrdU antibody. For intracellular cytokine staining, lung single cell suspensions were re-stimulated ex vivo in complete RPMI1640 media (supplemented with 10% FCS, 2 mM L-glutamine, 100 U/ml penicillin, 100 μg/ml streptomycin) containing 1 μg/ml ionomycin, 500 ng/ml PMA, and 10 μg/ml Brefeldin A for 4 hours at 37°C. Following surface staining and fixing, cells were intracellular stained with anti-IL-4 (11B11), IL-13 (eBio13A), IL-5 (TRFK5), and relevant isotypes. Expression of RELMα, Ym1, Arg-1, Ki67, IL-4, IL-13, and IL-5 was determined relative to isotype control staining. Incorporation of BrdU was determined relative to staining of non-DNase treated cells. Live/Dead (Life Technologies) was used to exclude dead cells from analysis.

Samples were analyzed by flow cytometry using Becton-Dickinson FACS LSR II and FlowJo software.

ELISAs

Quantification of RELMα (PeproTech, Rocky Hill, NJ) and Ym1 (R&D Systems) were performed by ELISA in BAL, pleural and peritoneal exudates, as well as in cell supernatants of *ex vivo* cultures of peritoneal or alveolar macrophages. IL-4, IL-5, IL-13, TNF-α, and IFN-γ (BioLegend and eBioscience) were measured in supernatants of *ex vivo* re-stimulated thoracic lymph node cells and liver homogenates. C1q quantification was performed by ELISA (Source BioScience, Nottingham, UK) in peritoneal cavity exudates. ELISA assays were performed following manufacturer instructions.

Isolation and culture of primary alveolar, peritoneal, and liver macrophages

Alveolar macrophages were obtained from BAL of mice and rats, and from human lung biopsies obtained from patients that were submitted to a lobectomy. An informed consent was obtained from all donors. The review board and the ethics committee of the Sabadell Hospital approved this study, which was conducted in accordance with the guidelines of the World Medical Association's Declaration of Helsinki. BAL was performed with Dulbecco's phosphate buffered saline with or without 0.2 mM EDTA and 0.5% BSA (m/v). Macrophages were purified by adherence for at least 90 min at 37°C, 5% CO_2 as previously reported (45). Adherent cells were 94.0 ± 1.1 % viable (trypan blue exclusion test). Flow cytometry analysis determined that 90 ± 1 % of adherent cells isolated from BAL were CD11c and SiglecF positive. To estimate the purity of isolated human macrophages, cells were cytospun in a CytoSpin 3 Cytocentrifuge (Shandon Scientific, Waltham, MA), and the cytospin preparations were stained either with anti-CD68 or Diff-Quick kit (Diagnostics Grifols, Barcelona, Spain) following the manufacturer's protocol. 95 % ± 1.5 % (n=6) of adherent cells were macrophages.

Peritoneal macrophages were obtained from mice by washing the peritoneal cavity with RPMI 1640 containing 2 mM L-glutamine, 200U/ml penicillin, 100 μg/ml streptomycin. For thioglycollate-induced macrophages, mice were injected with 0.4 ml of 4% Brewer's thioglycollate (Sigma) for 48–96 h before peritoneal cells were harvested. Cells were separated from the lavage fluid by centrifugation (250 x g, 5 min), resuspended in RPMI 1640 medium (5% heat-inactivated FBS, 100 U/ml penicillin, 100 μg/ml streptomycin, supplemented with glutamine 2 mM), and purified by adherence. Viability of adherent cells was assessed by trypan blue exclusion test. Flow cytometry analysis determined that 90 ± 1 % of adherent cell isolated from the peritoneal exudate were F4/80 and CD11b positive.

Liver macrophages were isolated from mouse livers as reported previously (46) with some modifications. Before collection of the tissue, mice were culled and bled by cutting the inferior vena cava. Subsequently the liver was perfused in situ with PBS. The liver was then excised and kept in HBSS. Subsequently, the organ was minced to small pieces and digested with collagenase B (0.2 mg/ml), collagenase D (0.4 mg/ml) (Roche) and 80 U/ml DNase (Life Technologies, Carlsbad, California) in HBSS at 37°C for 30 minutes. Digested tissue was filtered through a cell strainer (70 μm) to prepare a single cell suspension. The filtrate

was centrifuged twice at 300xg (4°C) for 5 min to wash out the residual enzymatic solution. The pellet was resuspended and centrifuged at 50xg (4°C) for 3 min to separate non-parenchymal from parenchymal cells. The pellet containing parenchymal cells was discarded. The supernatant was centrifuged again at 300xg for 5 min. The cell pellet was seeded on 96-well culture plates in complete culture medium [RPMI 1640 medium (10% heat-inactivated FBS, 100 U/ml penicillin, 100 μg/ml streptomycin, supplemented with glutamine 2 mM)]. Following incubation for 2 h in a humidified atmosphere of 95% air with 5% carbon dioxide (CO_2) at 37°C, the cells were gently washed with fresh culture medium. Viability of adherent cells was assessed by trypan blue exclusion test. Flow cytometry analysis determined that 70 ± 5 % of adherent cells isolated from the liver homogenates were F4/80 and CD11b positive.

In vitro stimulation of macrophages

Macrophages were pre-cultured for 24 h in RPMI 1640 medium with 5% FBS. Subsequently, cells were treated with IL-4 (0.5-1 μg/ml) (ImmunoTools, Berlin, Germany) and/or SP-A (25, 50 and 100 μg/ml) or native human C1q (10 and 100 μg/ml). The following blocking antibodies were added 2 hours before stimulation: 10 μg/ml of anti-Myo18A, 10-50 μg/ml anti-SIRPα (eBioscience), and 10-50 μg/ml anti-calreticulin (Thermo Scientific). Under these conditions cell viability was higher than 97%. Macrophage cultures were plated in triplicate wells and each series of experiments was repeated at least three times.

Cell proliferation assays

For 5–ethynyl–2′–deoxyuridine (EdU)/BrdU incorporation analysis, cells were treated with IL-4, SP-A, C1q and combinations thereof for 24 hours. Then, cells were exposed to 10 μM EdU/BrdU for another 24 hours. For confocal microscopy analysis of EdU incorporation, cells were fixed with 2% formaldehyde for 15 minutes at room temperature and permeabilized with 0.2% saponin in PBS. EdU was detected with Alexa Fluor 647-azide using Click-iT EdU assay kit (Life Technologies). Sequential double immunostaining was performed with a monoclonal antibody to CD11c (AbD Serotec, Kidlington, UK), and immune complexes were visualized with FITC-conjugated secondary antibody (Invitrogen). Micrographs were taken with a Leica TCS SP2 Confocal System. Flow cytometry analysis of BrdU and Ki67 expression was performed as described above.

Arginase activity assay

Arginase activity was measured as previously reported (47). Briefly, rat alveolar macrophages were lysed with 50 μl of 50 mM Tris–HCl pH 7.5, Triton X-100 0.1 %, 1 mM benzamidine, 200 μg/ml aprotinin, and 200 μg/ml leupeptin. After 30 min shaking at 4ºC, arginase was activated with 50 μl of 10 mM $MnCl_2$ and 50 mM Tris-HCl, pH 7.5, for 10 min at 55º C. L-arginine hydrolysis was measured by incubating the cell lysate with 25 μl of 0.5 M L-arginine (Sigma) (pH 9.7) at 37ºC for 1 h. The reaction was stopped by addition of 200 μl H_2SO_4 /H_3PO_4 /H_2O (1:3:7 v/v). The produced urea was quantified at 570 nm after addition of 25 μl of α-isonitrosopropiophenone (dissolved in 100% ethanol) followed by heating at 99ºC for 45 min. Urea production was normalized to cell number for each treatment by quantifying cells with the WST-1 reagent (Roche), following manufacturer'

instructions. One unit of arginase activity is defined as the amount of enzyme that catalyses the formation of 1 μmol urea per min.

siRNA-mediated gene-silencing effects in vitro

After isolation, primary alveolar macrophages were resuspended in Amaxa® mouse macrophage nucleofector solution (Lonza) and nucleofected with 100 nM siRNA using a nucleofector 2b device (Lonza). Experiments were conducted using two Stealth siRNAs directed against rat Myo18A (RSS322720 and RSS322721) (Applied Biosystems, Carlsbad, California). Medium GC Stealth siRNA was used as control (12935300) (Applied Biosystems). Myo18A expression was detected by Western blot analysis with an anti-Myo18A antibody. After 48 hours post nucleofection, Myo18A expression was reduced 72 ± 4% for RSS322720 and 71 ± 5% for RSS322721 compared to control. At this time-point, cells were stimulated.

Statistics

Normal distribution of data was determined by visual examination of residuals. Statistical evaluation of different groups was performed either by analysis of variance (ANOVA) followed by the Bonferroni multiple comparison test or by unpaired two-tailed Student's t-test, as indicated. An α level ≤ 5% ($p \leq 0.05$) was considered significant. All statistical calculations were performed using PRISM, (Graphpad La Jolla, CA).

Supplementary Material

Refer to Web version on PubMed Central for supplementary material.

Acknowledgements

The authors thank Martin Waterfall for expertise with flow cytometry; Marina Botto and Mohini Gray for providing $C1q^{-/-}$ mice; Cecile Benezech for providing IL-4R$\alpha^{-/-}$ mice; Sarah Walmsley for providing $LysM^{Cre/WT}$ / $HIF1\alpha^{fl/fl}$ mice; Dominik Rückerl, Mar Lorente, Rucha Tillu, for valuable advice; Gidona Goodman and Montserrat Rigol-Muxart for veterinary advice; Steve Jenkins for critical evaluation of the manuscript; Alison Fulton and Sheelagh Duncan for excellent technical assistance, and support staff for excellent animal husbandry.

C.M. Minutti was recipient of fellowships from the Spanish Ministry of Science (FPU- AP2010-1524 and Est13/00372) and Institute of Health Carlos III (CIBERES). This work was supported by the Spanish Ministry of Economy and Competitiveness (SAF2012-32728 and SAF2015-65307-R) and Institute of Health Carlos III (CIBERES-CB06/06/0002) to C. C., Medical Research Council UK (MR/K01207X/1) and Wellcome Centre for Cell-Matrix Research support to J. E. A., Medical Research Council (MR/M011755/1) and European Union (CIG-631413) to D.M.Z., and National of Institute Health grants HL068127 and HL128746 to Z. C.

References

1. Murray PJ, et al. Macrophage activation and polarization: nomenclature and experimental guidelines. Immunity. 2014; 41:14–20. [PubMed: 25035950]
2. Grencis RK. Immunity to helminths: resistance, regulation, and susceptibility to gastrointestinal nematodes. Annual review of immunology. 2015; 33:201–225.
3. Chen F, et al. An essential role for TH2-type responses in limiting acute tissue damage during experimental helminth infection. Nature medicine. 2012; 18:260–266.
4. Wynn TA, Vannella KM. Macrophages in Tissue Repair, Regeneration, and Fibrosis. Immunity. 2016; 44:450–462. [PubMed: 26982353]

5. Wright JR. Immunoregulatory functions of surfactant proteins. Nature reviews Immunology. 2005; 5:58–68.
6. Tenner AJ. Membrane receptors for soluble defense collagens. Current opinion in immunology. 1999; 11:34–41. [PubMed: 10047541]
7. Ruckerl D, Allen JE. Macrophage proliferation, provenance, and plasticity in macroparasite infection. Immunological reviews. 2014; 262:113–133. [PubMed: 25319331]
8. Goto H, et al. The role of surfactant protein A in bleomycin-induced acute lung injury. American journal of respiratory and critical care medicine. 2010; 181:1336–1344. [PubMed: 20167853]
9. Atochina EN, et al. Enhanced lung injury and delayed clearance of Pneumocystis carinii in surfactant protein A-deficient mice: attenuation of cytokine responses and reactive oxygen-nitrogen species. Infection and immunity. 2004; 72:6002–6011. [PubMed: 15385504]
10. Ledford JG, Pastva AM, Wright JR. Review: Collectins link innate and adaptive immunity in allergic airway disease. Innate immunity. 2010; 16:183–190. [PubMed: 20418258]
11. Minutti CM, et al. Surfactant Protein A Prevents IFN-gamma/IFN-gamma Receptor Interaction and Attenuates Classical Activation of Human Alveolar Macrophages. J Immunol. 2016; 197:590–598. [PubMed: 27271568]
12. Ikegami M, et al. Surfactant metabolism in SP-D gene-targeted mice. American journal of physiology. Lung cellular and molecular physiology. 2000; 279:L468–476. [PubMed: 10956621]
13. Thawer S, et al. Surfactant Protein-D Is Essential for Immunity to Helminth Infection. PLoS pathogens. 2016; 12:e1005461. [PubMed: 26900854]
14. Guzik-Lendrum S, et al. Mammalian myosin-18A, a highly divergent myosin. The Journal of biological chemistry. 2013; 288:9532–9548. [PubMed: 23382379]
15. De Masson A, et al. Identification of CD245 as myosin 18A, a receptor for surfactant A: A novel pathway for activating human NK lymphocytes. Oncoimmunology. 2016; 5:e1127493. [PubMed: 27467939]
16. Yang CH, et al. Identification of the surfactant protein A receptor 210 as the unconventional myosin 18A. The Journal of biological chemistry. 2005; 280:34447–34457. [PubMed: 16087679]
17. Petry F, Botto M, Holtappels R, Walport MJ, Loos M. Reconstitution of the complement function in C1q-deficient (C1qa-/-) mice with wild-type bone marrow cells. J Immunol. 2001; 167:4033–4037. [PubMed: 11564823]
18. Wang J, et al. The role of peritoneal alternatively activated macrophages in the process of peritoneal fibrosis related to peritoneal dialysis. International journal of molecular sciences. 2013; 14:10369–10382. [PubMed: 23685870]
19. Pletinck A, Vanholder R, Veys N, Van Biesen W. Protecting the peritoneal membrane: factors beyond peritoneal dialysis solutions. Nature reviews Nephrology. 2012; 8:542–550. [PubMed: 22777203]
20. Bellon T, et al. Alternative activation of macrophages in human peritoneum: implications for peritoneal fibrosis. Nephrology, dialysis, transplantation : official publication of the European Dialysis and Transplant Association - European Renal Association. 2011; 26:2995–3005.
21. Shipley JM, Wesselschmidt RL, Kobayashi DK, Ley TJ, Shapiro SD. Metalloelastase is required for macrophage-mediated proteolysis and matrix invasion in mice. Proceedings of the National Academy of Sciences of the United States of America. 1996; 93:3942–3946. [PubMed: 8632994]
22. Lu J, Wu X, Teh BK. The regulatory roles of C1q. Immunobiology. 2007; 212:245–252. [PubMed: 17544810]
23. Colegio OR, et al. Functional polarization of tumour-associated macrophages by tumour-derived lactic acid. Nature. 2014; 513:559–563. [PubMed: 25043024]
24. Watanabe S, et al. Serum C1q as a novel biomarker of sarcopenia in older adults. FASEB J. 2015; 29:1003–1010. [PubMed: 25491308]
25. Shi C, et al. Monocyte trafficking to hepatic sites of bacterial infection is chemokine independent and directed by focal intercellular adhesion molecule-1 expression. J Immunol. 2010; 184:6266–6274. [PubMed: 20435926]
26. Bleriot C, et al. Liver-resident macrophage necroptosis orchestrates type 1 microbicidal inflammation and type-2-mediated tissue repair during bacterial infection. Immunity. 2015; 42:145–158. [PubMed: 25577440]

27. Van Dyken SJ, Locksley RM. Interleukin-4- and interleukin-13-mediated alternatively activated macrophages: roles in homeostasis and disease. Annual review of immunology. 2013; 31:317–343.
28. Byrne AJ, Maher TM, Lloyd CM. Pulmonary Macrophages: A New Therapeutic Pathway in Fibrosing Lung Disease? Trends Mol Med. 2016; 22:303–316. [PubMed: 26979628]
29. Xue J, et al. Alternatively activated macrophages promote pancreatic fibrosis in chronic pancreatitis. Nat Commun. 2015; 6:7158. [PubMed: 25981357]
30. Coya JM, et al. Natural Anti-Infective Pulmonary Proteins: In Vivo Cooperative Action of Surfactant Protein SP-A and the Lung Antimicrobial Peptide SP-BN. J Immunol. 2015; 195:1628–1636. [PubMed: 26163587]
31. Garcia-Verdugo I, Sanchez-Barbero F, Bosch FU, Steinhilber W, Casals C. Effect of hydroxylation and N187-linked glycosylation on molecular and functional properties of recombinant human surfactant protein A. Biochemistry. 2003; 42:9532–9542. [PubMed: 12911295]
32. Sanchez-Barbero F, Rivas G, Steinhilber W, Casals C. Structural and functional differences among human surfactant proteins SP-A1, SP-A2 and co-expressed SP-A1/SP-A2: role of supratrimeric oligomerization. The Biochemical journal. 2007; 406:479–489. [PubMed: 17542781]
33. Sanchez-Barbero F, Strassner J, Garcia-Canero R, Steinhilber W, Casals C. Role of the degree of oligomerization in the structure and function of human surfactant protein A. The Journal of biological chemistry. 2005; 280:7659–7670. [PubMed: 15615713]
34. Li G, et al. Surfactant protein-A--deficient mice display an exaggerated early inflammatory response to a beta-resistant strain of influenza A virus. American journal of respiratory cell and molecular biology. 2002; 26:277–282. [PubMed: 11867335]
35. Carlucci F, et al. C1q Modulates the Response to TLR7 Stimulation by Pristane-Primed Macrophages: Implications for Pristane-Induced Lupus. J Immunol. 2016; 196:1488–1494. [PubMed: 26773156]
36. Herbert DR, et al. Alternative macrophage activation is essential for survival during schistosomiasis and downmodulates T helper 1 responses and immunopathology. Immunity. 2004; 20:623–635. [PubMed: 15142530]
37. Thompson AA, et al. Hypoxia-inducible factor 2alpha regulates key neutrophil functions in humans, mice, and zebrafish. Blood. 2014; 123:366–376. [PubMed: 24196071]
38. Jenkins SJ, et al. Local macrophage proliferation, rather than recruitment from the blood, is a signature of TH2 inflammation. Science. 2011; 332:1284–1288. [PubMed: 21566158]
39. Jenkins SJ, et al. IL-4 directly signals tissue-resident macrophages to proliferate beyond homeostatic levels controlled by CSF-1. The Journal of experimental medicine. 2013; 210:2477–2491. [PubMed: 24101381]
40. Jackson-Jones LH, et al. IL-33 delivery induces serous cavity macrophage proliferation independent of interleukin-4 receptor alpha. Eur J Immunol. 2016; 46:2311–2321. [PubMed: 27592711]
41. Camberis M, Le Gros G, Urban J Jr. Animal model of Nippostrongylus brasiliensis and Heligmosomoides polygyrus. Current protocols in immunology / edited by John E. Coligan ... [et al.]. 2003; Chapter 19 Unit 19 12.
42. Holland MJ, Harcus YM, Riches PL, Maizels RM. Proteins secreted by the parasitic nematode Nippostrongylus brasiliensis act as adjuvants for Th2 responses. Eur J Immunol. 2000; 30:1977–1987. [PubMed: 10940887]
43. Sutherland TE, et al. Chitinase-like proteins promote IL-17-mediated neutrophilia in a tradeoff between nematode killing and host damage. Nature immunology. 2014; 15:1116–1125. [PubMed: 25326751]
44. Samten B, et al. An antibody against the surfactant protein A (SP-A)-binding domain of the SP-A receptor inhibits T cell-mediated immune responses to Mycobacterium tuberculosis. Journal of leukocyte biology. 2008; 84:115–123. [PubMed: 18443188]
45. Casals C, et al. Surfactant strengthens the inhibitory effect of C-reactive protein on human lung macrophage cytokine release. American journal of physiology. Lung cellular and molecular physiology. 2003; 284:L466–472. [PubMed: 12573986]
46. Zeng WQ, et al. A new method to isolate and culture rat kupffer cells. PLoS One. 2013; 8:e70832. [PubMed: 23967115]

47. MacKinnon AC, et al. Regulation of alternative macrophage activation by galectin-3. J Immunol. 2008; 180:2650–2658. [PubMed: 18250477]

Europe PMC Funders Author Manuscripts

Europe PMC Funders Author Manuscripts

One Sentence Summary

Specific signals within the tissues are required to enhance IL-4Rα mediated macrophage activation and proliferation during infection and injury.

Europe PMC Funders Author Manuscripts

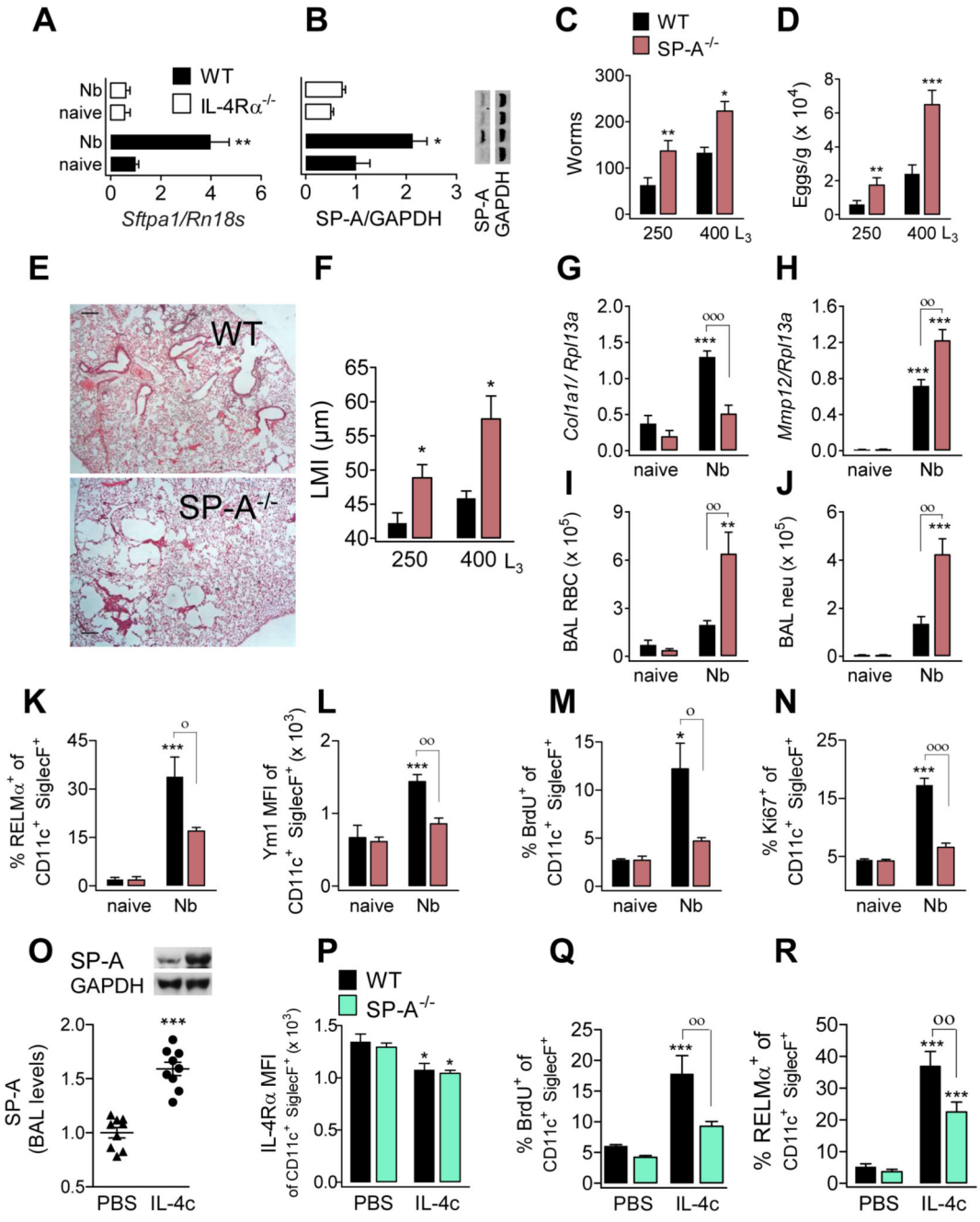

Fig. 1. Higher worm burden, greater nematode-induced lung damage and reduced IL-4-induced proliferation and activation in mice lacking SP-A.

Samples were assessed at d6 after *N. brasiliensis* infection. SP-A **(A)** mRNA and **(B)** protein expression in lung tissue of WT and IL-4Rα$^{-/-}$ mice. **(C)** Adult larvae in the small intestine, **(D)** egg output in faeces, and **(E)** microscopy of H&E stained lung sections (scale bars, 500 μm) in WT and SP-A$^{-/-}$ mice. **(F)** Lung damage, quantified by 'mean linear intercept' from micrographs of H&E stained lung sections. **(G)** Amplification of *Col1a1*- and **(H)** *Mmp12*-encoding mRNA in lung tissue. Number of **(I)** red blood cells and **(J)** neutrophils isolated in

BAL. Expression of **(K)** RELMα and **(L)** Ym1 by aMϕ from BAL. Because all aMϕ are Ym1 positive, MFI is shown for Ym1. **(M)** BrdU incorporation and **(N)** Ki67 expression by aMϕ from BAL. Data are representative from two independent experiments (mean ± SEM; naïve: 3 mice, *Nb*: 6 mice). (**O-R)** WT and SP-A$^{-/-}$ mice treated with 5μg IL-4c (i.p.) at days 0 and 2 and analyzed at day 4. **(O)** Relative SP-A levels in BAL (representative western blot shown) of WT mice treated with IL-4c or PBS. **(P)** Expression of IL-4Rα by aMϕ from BAL. **(Q)** BrdU incorporation and **(R)** RELMα expression in aMϕ. Data pooled from three independent experiments (means ± SEM) (PBS: 9 mice, IL-4c: 11 mice). ANOVA followed by the Bonferroni multiple-comparison test was used. *$p < 0.05$, **$p < 0.01$, and ***$p < 0.001$ when compared with the untreated/uninfected group. °$p < 0.05$, °°$p < 0.01$ and °°°$p < 0.001$ when WT vs. SP-A$^{-/-}$ groups are compared.

Europe PMC Funders Author Manuscripts

Europe PMC Funders Author Manuscripts

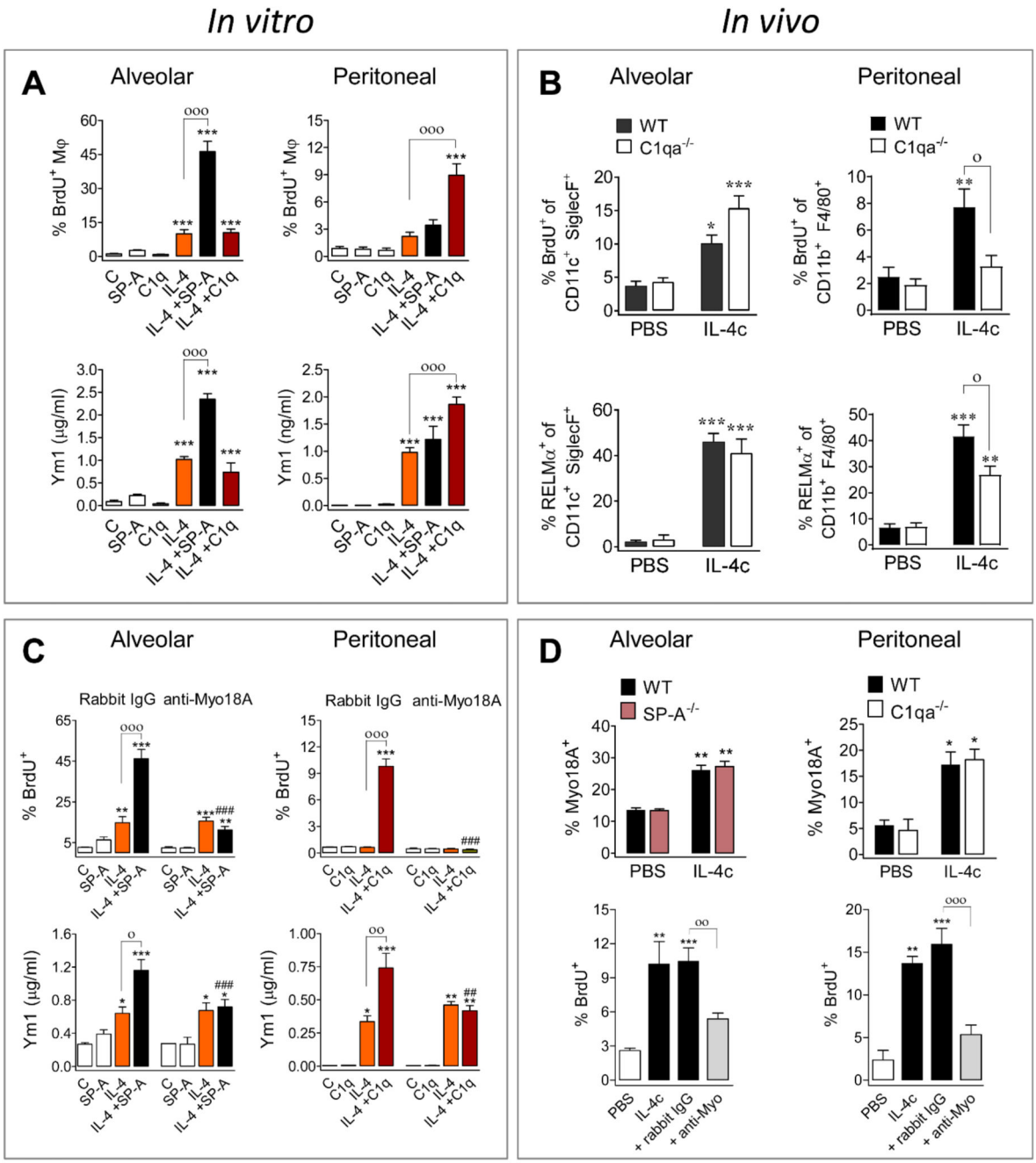

Fig. 2. SP-A and C1q act through Myo18A to enhance IL-4-induced proliferation and activation of alveolar and peritoneal macrophages, respectively.

(A) Murine macrophages were treated with IL-4 in the presence or absence of SP-A or C1q. BrdU incorporation and secretion of Ym1 are shown. **(B)** For aMϕs, 5 μg IL-4c was delivered ip at d0 and d2, and BAL cells analyzed at d4. For pMϕs, 1 μg IL-4c was delivered ip at d0, and peritoneal cells analyzed at d1: BrdU incorporation and RELMα expression are shown. **(C)** Murine macrophages were treated with anti-Myo18A or rabbit IgG plus either IL-4+SP-A (aMϕ) or IL-4+C1q (pMϕ). BrdU incorporation and secretion of Ym1 are

shown. **(D)** Myo18A expression on the surface of macrophages from WT, SP-A$^{-/-}$, and C1qa$^{-/-}$ mice treated with or without IL-4c as described in (B). Concurrently with IL-4c delivery, some WT mice were intra-nasally treated with either anti-Myo18A or rabbit IgG antibody at d2 and d3, and samples analyzed at d4. BrdU incorporation is shown. All statistical analysis was performed by ANOVA followed by the Bonferroni multiple-comparison test. (A+C) Results are presented as means (± SEM) from three different cell cultures with at least three biological replicates. *$p < 0.05$, **$p < 0.01$, and ***$p < 0.001$, when compared with untreated cells; °$p < 0.05$, °°$p < 0.01$, and °°°$p < 0.001$, when SP-A +IL-4- or C1q+IL4-treated are compared with IL-4-treated; ##$p < 0.01$, and ###$p < 0.001$, the effect of anti-Myo18A antibody on cells treated with SP-A+IL-4 or C1q+IL4. (B+D) Data were pooled from three independent experiments (means ± SEM) (PBS: 6 mice, other groups: 9 mice). *$p < 0.05$, **$p < 0.01$, and ***$p < 0.001$, when compared with PBS treated mice; °$p < 0.05$, when WT vs. C1qa$^{-/-}$ mice treated with IL-4c are compared (B) °$p < 0.05$, °°$p < 0.01$, and °°°$p < 0.001$ when anti-Myo18A vs rabbit IgG treatment is compared in IL-4c-treated mice (D).

Europe PMC Funders Author Manuscripts

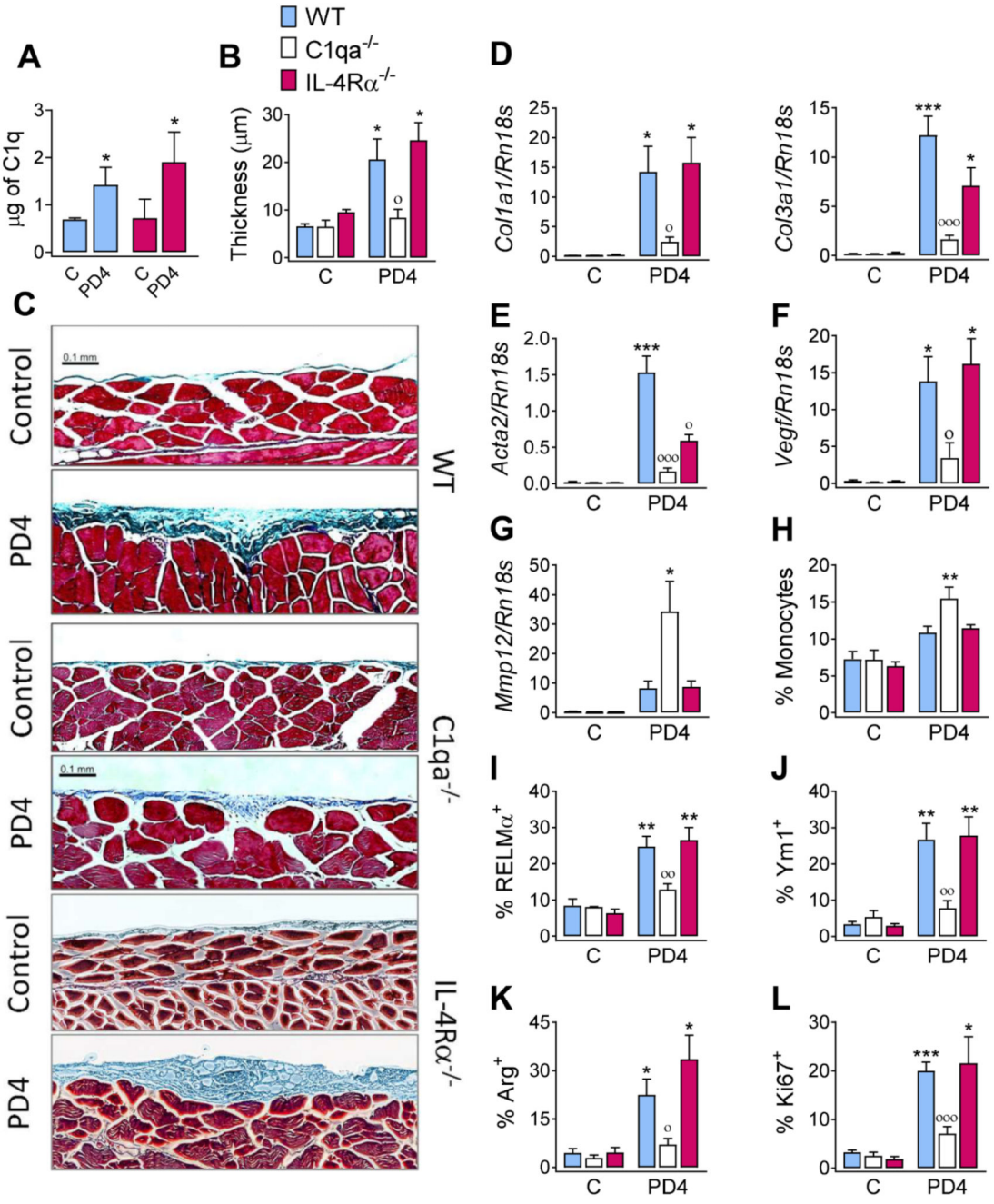

Fig. 3. C1q enhances peritoneal fibrosis induced by a lactate dialysate.

WT, C1qa$^{-/-}$ or IL-4Rα$^{-/-}$ mice were either untreated (C) or treated with a 14 ip injections of Dianeal PD-4 every other day. Samples were analyzed a day after the last delivery. **(A)** Total amount of C1q in the peritoneal washes was determined by ELISA. **(B)** Quantification of the thickness of the submesothelial compact zone from **(C)** microscopy of Masson's trichrome stained parietal peritoneum slices (scale bars, 0.1 mm). Amplification of **(D)** *Col1a1, Col3a1*, **(E)** *Acta2*, **(F)** *Vegf*, and **(G)** *Mmp12*-encoding mRNA in peritoneal tissue. **(H)** Percentage of infiltrating monocytes as quantified by FACS. Expression of **(I)** RELMα, **(J)**

Ym1, **(K)** Arg and **(L)** Ki67 by peritoneal macrophages. Results are representative from two independent experiments (means ± SEM) (untreated: 3 mice, PD4: 6 mice). ANOVA followed by the Bonferroni multiple-comparison test or Student's *t*-test (A) was used. $*p < 0.05$, $**p < 0.01$, and $***p < 0.001$ when compared with control group; $°p < 0.05$, $°°p < 0.01$, and $°°°p < 0.001$ when WT vs. $C1qa^{-/-}$ mice treated with Dianeal PD-4 are compared.

Europe PMC Funders Author Manuscripts

Europe PMC Funders Author Manuscripts

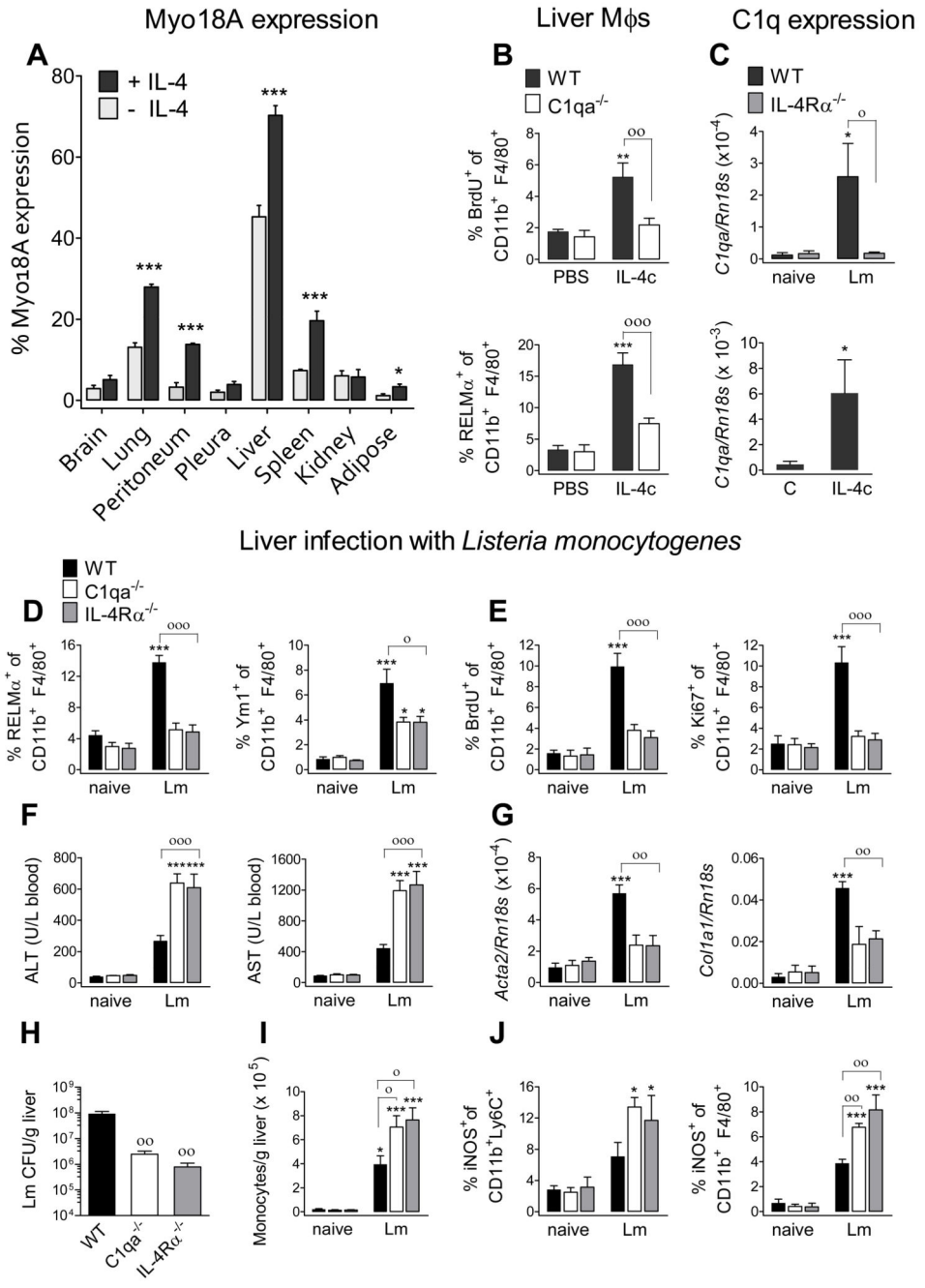

Fig. 4. C1q is required for appropriate macrophage activation in the liver during *Listeria monocytogenes* infection.

(A, B, C) WT or C1qa$^{-/-}$ mice received 1 μg IL-4c (ip) at d0, and samples were analyzed at d1. **(A)** Myo18A expression on the surface of resident macrophages from the indicated tissues. Resident macrophages were identified as described in the methods **(B)** BrdU incorporation and RELMα expression of liver macrophages. **(C)** (lower panel) IL-4-induced amplification of *C1q*-encoding mRNA in the liver. **(C-J)** WT, C1qa$^{-/-}$, or IL-4Rα$^{-/-}$ mice were left uninfected or received intravenous infection with 10^4 *L. monocytogenes* c.f.u. and

samples were assessed at 3.5 dpi. **(C)** (upper panel) Lm-induced amplification of *C1q*-encoding mRNA. (**D**) Expression of RELMα and Ym1 by liver macrophages. **(E)** BrdU incorporation and Ki67 expression by liver macrophages. **(F)** Quantification of ALT and AST in serum. **(G)** Amplification of *Acta2*- and *Col1a1*-encoding mRNA in the liver. **(H)** Liver bacterial load. **(I)** Number of monocytes in liver single cell suspensions. **(J)** iNOS expression by liver monocytes and macrophages. Data are representative from two independent experiments (mean ± SEM; naïve: 4 mice, *Lm*: 5 mice). ANOVA followed by the Bonferroni multiple-comparison test was used. $*p < 0.05$, and $***p < 0.001$, when compared with the uninfected group; $°p < 0.05$, $°°p < 0.01$, and $°°°p < 0.001$ when WT vs. C1qa$^{-/-}$ or IL-4Rα$^{-/-}$ infected groups are compared.

Europe PMC Funders Author Manuscripts